NACA

RESEARCH MEMORANDUM

ROCKET-POWERED-MODEL INVESTIGATION OF THE HINGE-MOMENT AND NORMAL-FORCE CHARACTERISTICS OF A HALF-DIAMOND TIP CONTROL ON A 60° SWEPTBACK DIAMOND WING BETWEEN MACH NUMBERS OF 0.5 AND 1.3

By James D. Church

Langley Aeronautical Laboratory
Langley Field, Va.

NATIONAL ADVISORY COMMITTEE
FOR AERONAUTICS

WASHINGTON

April 26, 1954

[redacted]

Classification cancelled (or changed to UNCLASSIFIED)

By Authority of NASA Tech Pub Announcement #62
(OFFICER AUTHORIZED TO CHANGE)

By [redacted]
NAME AND

[redacted]
GRADE OF OFFICER MAKING CHANGE)

3 Apr 61
DATE

iQ

NACA RM L54C10

NATIONAL ADVISORY COMMITTEE FOR AERONAUTICS

RESEARCH MEMORANDUM

ROCKET-POWERED-MODEL INVESTIGATION OF THE HINGE-MOMENT AND NORMAL-FORCE CHARACTERISTICS OF A HALF-DIAMOND TIP CONTROL ON A 60° SWEPTBACK DIAMOND WING BETWEEN MACH NUMBERS OF 0.5 AND 1.3

By James D. Church

SUMMARY

A free-flight investigation has been conducted to determine normal-force and hinge-moment characteristics of a half-diamond tip control on a diamond wing having 60° sweptback leading edges and 30° sweptforward trailing edges through a range of Mach numbers of 0.5 to 1.3. Results indicate that the control could be so hinged that very small hinge-moments due to control deflection would be obtained at low angles of attack over the speed range tested, although nonlinear variations of hinge moment with angle of attack were present in the transonic range.

The center of pressure of the control-deflection forces had subsonic and supersonic locations of about 35 and 40 to 45 percent control mean aerodynamic chord, respectively, with angle of attack affecting only the lower supersonic region. The center of pressure of the control forces due to model angle of attack had mean subsonic and supersonic locations of about 31 and 41 percent chord.

Control normal force per unit deflection was roughly half as large as control normal force per unit angle of attack. At supersonic speeds only 10 to 30 percent of the total normal force developed by control deflection was induced on the wing-model combination.

A comparison of control-wing plan forms showed that a half-diamond shape had more control normal force per unit angle of attack and a more forward center of pressure of the control-deflection force than a half-delta shape over the speed range investigated.

INTRODUCTION

Recent evaluation of the results from numerous research investigations of various control devices (ref. 1) indicates the desirability of further study of tip controls. In order to obtain more data on the force and moment characteristics of a previously tested control of this type (ref. 2), an investigation was conducted through the use of a rocket-powered model incorporating 60° sweptback diamond wings having 30° sweptforward trailing edges with half-diamond tip elevators of matching plan form.

Control hinge moments were continuously measured about two hinge-line locations on one model at various angles of attack (ranging from ±3° to ±14°) and control deflections (up to ±13°) between Mach numbers 0.50 and 1.30. The magnitude and chordwise position of control normal force were determined as separate functions of angle of attack and control deflection by using faired hinge-moment coefficients.

Lift effectiveness data for the controls and the entire model were also obtained. These results are presented herein and compared with other rocket-powered-model data.

SYMBOLS

b	wing span, 2.252 ft
$\bar{c}$	wing mean aerodynamic chord, 1.725 ft
c_a	control root chord, 0.625 ft
$\bar{c}_a$	control mean aerodynamic chord, 0.417 ft
S	total wing area in one plane, 2.909 sq ft
S_a	area of one control surface, 0.0850 sq ft
δ	control-surface deflection (trailing edge down, positive), deg
α	angle of attack at model center of gravity, deg
A	wing aspect ratio, $\frac{b^2}{S} = 1.743$
M	Mach number

[redacted]

V free-stream velocity, ft/sec

q dynamic pressure, lb/sq ft

R Reynolds number (based on $\bar{c}$)

a_n model normal acceleration, g units

g acceleration due to gravity, 32.2 ft/sec/sec

H hinge moment of one control about hinge line, in-lb

C_h control hinge-moment coefficient, $\frac{H/12}{qS_a\bar{c}_a}$

C_N total normal-force coefficient, $\frac{\text{Normal force on model}}{qS}$

$(C_N)_a$ control normal-force coefficient, $\frac{\text{Normal force on control surface}}{qS_a}$

c.p.$_\delta$ chordwise center-of-pressure location of the control force due to control deflection, percent $\bar{c}_a$

c.p.$_\alpha$ chordwise center-of-pressure location of the control force due to angle of attack, percent $\bar{c}_a$

$$C_{h_\delta} = \frac{\partial C_h}{\partial \delta}$$

$$C_{h_\alpha} = \frac{\partial C_h}{\partial \alpha}$$

$$C_{N_\delta} = \frac{\partial C_N}{\partial \delta}\frac{S}{2S_a}$$

$$C_{N_\alpha} = \frac{\partial C_N}{\partial \alpha}$$

$$(C_{N_\delta})_a = \frac{\partial (C_N)_a}{\partial \delta}$$

[redacted]

$$(c_{N\alpha})_a = \frac{\partial(c_N)_a}{\partial\alpha}$$

Subscripts:

1 refers to control with hinge line at $0.5073c_a$

2 refers to control with hinge line at $0.5561c_a$

MODEL AND INSTRUMENTATION

The hinge-moment research model used in this investigation consisted of a cylindrical body, with ogival nose and tail sections, equipped with a cruciform arrangment of aspect-ratio-1.74 diamond wings. These wings had 60° sweptback leading edges and 30° sweptforward trailing edges. A drawing of the model showing overall dimensions is presented in figure 1 and photographs of the model are shown in figure 2.

The wing panels in one plane were equipped with half-diamond tip controls, the ratio of total control area to total exposed wing area in one plane (including control area) being 1/9.4. The magnesium-alloy wing panels had a modified hexagonal airfoil section of constant maximum thickness, the maximum-thickness ratio of which varied from 2.94 percent at the wing-body junction to 9.03 percent at the parting line of the wing and tip control. The tip controls, fastened to the outboard ends of torque rods, had double-wedge airfoil sections modified by a rounded leading edge with a constant ratio of maximum thickness to chord of 3 percent. One control was hinged at $0.5073c_a$ ($0.3860\bar{c}_a$) and the other control was hinged at $0.5561c_a$ ($0.4592\bar{c}_a$); the hinge lines were located within the wing such that the wing-control combinations formed continuous plan forms. The controls were of solid steel construction and the parting line gap was 0.036 inch. Figure 3 shows the dimensions of the wing and tip controls.

The model had an NACA telemetering system which transmitted the normal, transverse, and longitudinal acceleration, the static and total pressure, the deflection angle and hinge moments of each control, the angle of attack, and the rate of pitch. A control-position indicator and balances to measure control-hinge moments were constructed as integral parts of a power unit mounted in the rear of the model wing section.

In addition to this instrumentation, a radiosonde recorded atmospheric data at all flight altitudes shortly after the flight. Flight-path data were obtained with a radar tracking unit and a CW Doppler radar set was used to determine initial flight velocities. Photographic tracking was also employed to obtain visual records of the flight.

TECHNIQUE AND ACCURACY

The technique employed in this investigation consisted of mechanically pulsing the controls as elevators throughout the flight so that their deflection varied sinusoidally with time. The pulsing frequency was varied from 4.7 cycles per second at a Mach number of 1.33 to 1.4 cycles per second at a Mach number of 0.50 in an attempt to produce a nearly constant phase lag between the model pitching response and the control input. The control pulsing amplitude varied from $\pm 9^\circ$ to $\pm 13^\circ$ because of varying deflections in the control linkage throughout the speed range.

In addition to the aforementioned pitching oscillations, the response of the model involved small rolling and sideslip oscillations, the rolling motion being minimized by a built-in incremental difference in the deflection ranges of the two controls. The effects of these small oscillations (maximum angle of sideslip was approximately 1.1° at $M = 0.70$) are believed to be negligible upon the results. This technique allowed continuous measurements of hinge moments for each of the controls at various combinations of control deflection and angle of attack over the Mach number range of the investigation.

From separate measurements of the variation of hinge moments with control deflection and angle of attack for each of the controls and a knowledge of the chordwise location of the hinge lines, the chordwise location and magnitude of the control normal forces (assumed independent of hinge-line location) were determined as independent functions of angle of attack and control deflection. All hinge-moment data were corrected for inertia effects of the control and control linkage caused by the pulsing motion.

The following information has been tabulated to indicate possible errors in the basic measurements.

Hinge moment, in-lb	± 1.10
Control deflection, deg	± 0.20
Angle of attack, deg	± 0.26
Normal acceleration, g units	± 0.40

These values are representative of the maximum instrument error in evaluating isolated data. In computations involving differences (such as slope evaluation), possible errors in the component quantities can be considered to be roughly one-half as large as those indicated.

The largest error introduced by considering one cycle of information to be at a constant Mach number was of the order of $\Delta M = 0.03$. A more detailed description of the technique employed and the sources of error therein is given in references 3 and 4.

[redacted]

The test variations of Reynolds number and dynamic pressure with Mach number are presented in figure 4. All data were obtained in decelerated flight (0g to -3.0g). The small test-point scatter and out-of-trim component of the hinge-moment-coefficient data indicate that the probable repeatability error of these measurements would be much smaller than computed from the preceding table and figure 4.

RESULTS AND DISCUSSION

Control Hinge Moments

As previously stated, hinge moments were measured on two nominally identical control surfaces on a single model varying only in hinge-line location. (See fig. 3(b).) Simultaneous values of the recorded angle of attack, control-surface deflection, and control hinge-moment coefficient for both controls at various Mach numbers are presented in table I.

A sample plot of the basic data is shown in figure 5. The solid-line curve connecting the data points represents the measured hinge-moment-coefficient data, and the straight lines (fig. 5(a)) which connect end points of equal angle of attack were constructed by assuming C_{h_δ} to be constant with δ at individual angles of attack so as to obtain some indication of the separate effects of α and δ on control forces and hinge moments. Since this assumption could introduce considerable error, especially at the higher angles of attack and in the transonic speed region, the results obtained should be considered mainly as trends. (See ref. 3.) Regardless of the fairing employed for any further analysis of the data, the important result is that all hinge moments measured were small over the speed range for the size control tested.

Cross-plotting the faired C_h intercepts at various deflections as a function of angle of attack yields the constant-deflection curves of figure 5(b), and since this form of data presentation more readily illustrates the hinge-moment nonlinearities with respect to angle of attack, all data were plotted in this form. In this regard, the data can be plotted in any manner the reader desires by using table I; this table contains all the measured points for $M = 0.80$ through $M = 1.30$ and about 50 percent of the test points available for Mach numbers of 0.50, 0.60, and 0.70. (Some additional Mach numbers in the transonic region have been omitted.)

Hinge-moment coefficients were determined for all combinations of angle of attack and control deflection within the data loops at each Mach number by linear interpolation between the curves of constant control deflection. Similarly, reasonable extrapolation (about half the

data loop width in the C_h direction beyond the test points as shown in figure 5(b)) yielded values outside the data loops. Data obtained in such a manner are shown for several Mach numbers in figure 6. If the assumption of a linear C_{h_δ} is invalid, the shape of the curves in figure 6 would change, especially over the region of the dashed portions of these curves. Regardless of the extent of these nonlinearities, the order of magnitude of C_h at any α and δ would be substantially unchanged.

C_{h_δ}.- The parameter C_{h_δ} is indicated by the incremental displacement between the constant-deflection curves of figure 6 (identical to slope of constant-angle-of-attack lines of figure 5(a)), where negative values of C_{h_δ} indicate the control to be statically stable with deflection, that is, the center of pressure of the deflection loading is behind the hinge line. For the forward hinge line ($0.5073C_a$), values of C_{h_δ} are positive at all angles of attack for $M = 0.70$ and negative for $M = 0.95$ and 1.10, angle of attack having the greatest effect at $M = 0.95$.

The values of C_{h_δ} are presented as a function of Mach number in figure 7 for each of the test hinge lines at angles of attack of 0° and 3°. These values are relatively small at all speeds for both hinge lines. All the curves are seen to be rather constant at subsonic Mach numbers with an abrupt negative shift as Mach number increases from 0.90 to 0.95, the curves at angle of attack having a more negative shift in this region. It should be pointed out, however, that the rate of change of C_{h_δ} with angle of attack was nonlinear in the region between $\alpha = 4^\circ$ and $\alpha = -4^\circ$, particularly at transonic speeds.

C_{h_α}.- The reader can see the effects of angle of attack on hinge moments in figure 6; in this figure, the slope of the constant-deflection curves for various control deflections indicates the parameter C_{h_α}. The variation of C_{h_α} with angle of attack, for the forward hinge line, can be seen to be nearly constant up to values of α of $\pm 3^\circ$ or $\pm 4^\circ$ at $M = 0.70$ and 1.10 and was nonlinear over the entire measured angle-of-attack range for all deflections at $M = 0.95$.

Values of C_{h_α} are presented in figure 8 as a function of Mach number for each of the two test hinge lines. The values represent faired slopes near $\alpha = 0$ and incremental slopes over an angle-of-attack range of $\pm 3^\circ$ and were obtained at zero control deflection. Although the curves have a similar variation with Mach number, the rearward hinge line retained a positive value at all speeds, whereas the forward hinge line had a

positive C_{h_α} subsonically and a negative value at supersonic speeds. Thus, the variation of C_{h_α} indicates that the center of pressure of the control angle-of-attack loading remained forward of the test hinge lines through the transonic range and then moved between the control pivot axes over the tested supersonic range. In general, increasing the α range to $\pm 3^\circ$ resulted in a smoother variation of C_{h_α} with Mach number.

It should be noted that the variation of hinge-moment coefficient with either control deflection or angle of attack for hinge-line locations other than those tested can be obtained by linear interpolation or extrapolation of the results presented in figures 7 and 8 at any constant Mach number. For purposes of further analysis, the hinge-moment-coefficient data were reduced to control-force data (determined from the assumed linear relationship between C_{h_δ} or C_{h_α} and the chordwise hinge-line location) which are discussed in the subsequent section.

CONTROL NORMAL FORCE

The variations with Mach number of the control normal-force-coefficient slope and chordwise center-of-pressure location with respect to both angle of attack and control deflection are presented in figures 9 and 10 between Mach numbers of 0.50 and 1.30.

$(C_{N_\delta})_a$.- The control normal-force-coefficient slope with control deflection evaluated at $\alpha = 0$ is seen to vary smoothly over the Mach number range with a maximum value of 0.048 occurring at $M = 0.95$. (See fig. 9(a).) Other rocket test data (ref. 3) for a half-delta tip control indicate that this parameter was not materially affected by the difference in the two tested plan forms. Angle of attack affected $(C_{N_\delta})_a$ in two different ways. At supersonic speeds, a slight reduction in normal-force coefficient was measured for $\alpha = \pm 3^\circ$; however, in the subsonic region, $\alpha = -3^\circ$ increased and $\alpha = 3^\circ$ decreased $(C_{N_\delta})_a$. (These effects were of the same order as the difference between the present test and ref. 3 for the entire speed range investigated.)

c.p.$_\delta$.- Variations with Mach number of the center of pressure of the control force resulting from control deflection are shown in figure 9(b) for reference 3 and for the present test at angles of attack of 0°, 3°, and -3°. The curve for $\alpha = 0$ shows that c.p.$_\delta$ had a

basic subsonic position of about 35 percent mean aerodynamic chord ($\bar{c}_a$) that moved abruptly rearward about 5 to $5\frac{1}{2}$ percent between the Mach numbers of 0.87 to 0.98 and a supersonic location that increased from approximately $40\frac{1}{2}$ to $45\frac{1}{2}$ percent $\bar{c}_a$. The principal effect of angle of attack was an irregular rearward shift of this variable at transonic and supersonic speeds. The difference in the amount of shift between the curves for $\alpha = 3^\circ$ and $\alpha = -3^\circ$ at subsonic speeds points out the apparent asymmetry mentioned previously. A comparison of the present test and reference 3 indicates the main difference in c.p.$_\delta$ was a forward shift (approximately 4 percent for $M < 0.85$ and 7 to 3 percent for $1.00 < M < 1.30$) for the half-diamond control with respect to the half-delta control.

Since rather involved computations are necessary in the evaluation of the pressure distribution by linear theory for a control of the plan form tested, it was decided that only a very general comparison of theory with experiment was within the scope of the present paper. In this connection, if the controls are considered as isolated half-plan forms, the theories of references 5 and 6 prove of value in determining the validity of the trends shown in figure 9(b). In the subsonic range, the experimental difference between the two tested plan forms for $\alpha = 0$ is exactly opposite to that which is anticipated from low-aspect-ratio considerations (ref. 5); this fact indicates that the influence of the wing upon the flow over the control and the flow through the streamwise gap at the control root chord are of sufficient magnitude to reverse the trend of the theoretical prediction. At transonic and supersonic speeds, however, the experimental trend of the two plan forms is in good agreement with theory (see ref. 6); near $M = 1.00$, the forward c.p.$_\delta$ shift for the half-diamond control being caused by the region of low pressure occurring behind the shock wave stemming from the control tip and, as the Mach number increases, the c.p.$_\delta$ approaches that of the half-delta surface because of the reduction of this region of low pressure as the shock moves toward the trailing edge. With regards to the effect of $\alpha = \pm 3^\circ$ on these results, it is quite conceivable theoretically that at supersonic speeds the region of lifting pressure induced on the control by the wing could more than offset the region of pressure loss across the control apex shock and result in a rearward c.p.$_\delta$ shift for the half-diamond control compared with its $\alpha = 0$ position.

$(C_{N_\alpha})_a$.- The slope of the control-normal-force-coefficient curve with angle of attack has been plotted against Mach number in figure 10(a). These values, obtained at $\delta = 0$, were determined over the same angle-of-attack ranges as presented in figure 8. The test curves are smooth and show that values of this variable are at least twice as large as comparable values of $(C_{N_\delta})_a$, with the curve for $\alpha = \pm 3^\circ$ being approximately

0.01 higher than the curve for $\alpha = 0$ at transonic and supersonic speeds (again illustrating the nonlinear nature of the angle-of-attack effects). A comparison of the results of the present test and reference 3 shows that although the controls have similar trends with Mach number, the half-diamond tip control had more angle-of-attack loading than the half-delta tip control for a similar angle-of-attack range.

c.p.$_\alpha$.- The chordwise location of the control normal force due to angle of attack is shown in figure 10(b) as a function of Mach number for the same angle-of-attack ranges as its counterpart $(C_{N_\alpha})_a$. From a mean subsonic value of 31 percent $\bar{c}_a$, c.p.$_\alpha$ for α approaching zero is seen to increase to a mean value of 41 percent $\bar{c}_a$ at supersonic speeds; c.p.$_\alpha$ was 3 to 4 percent $\bar{c}_a$ forward of c.p.$_\delta$. The importance of the angle-of-attack range employed in evaluating c.p.$_\alpha$ is illustrated by the 1 to 2 percent $\bar{c}_a$ change in this parameter over the Mach number range for $\alpha = \pm 3^\circ$. It is now apparent that the irregular variations of C_{h_α} (fig. 8) and c.p.$_\delta$ ($\alpha = \pm 3^\circ$) with Mach number are due almost entirely to variations in c.p.$_\alpha$. A subsonic rearward movement of c.p.$_\alpha$ represents the primary trend resulting from changing the control plan form (comparison of present test and ref. 3) from a half-delta to a half-diamond shape, the effect at other speeds being very irregular (maximum change at all speeds was of the order of $2\frac{1}{2}$ percent $\bar{c}_a$).

TOTAL NORMAL FORCE

C_{N_α} and C_{N_δ}.- The slope of the model normal-force coefficient with respect to control deflection and angle of attack was determined from normal accelerations measured throughout the flight in the same manner as the hinge-moment slopes. Since the lines of constant angle of attack (similar to fig. 5(a)) were nearly parallel and equally spaced along the C_N axis, the values of C_{N_δ} and C_{N_α} are independent of angle of attack and control deflection, respectively. These results are presented in figure 11(a) as a function of Mach number and are compared with the results from reference 3. The C_{N_α} values of the present test (A = 1.74) are smaller than the differences in aspect ratio would lead one to expect and have a similar variation with Mach number as those for the delta-wing model of reference 3 (A = 2.35). The principal difference between C_{N_δ} for the two tests was the higher subsonic values for the delta plan form.

Control "carry over".- The C_{N_δ} curve (based on control area), which represents the total normal force developed by control deflection at a

fixed angle of attack, includes the normal forces induced on the model and wing by control deflection as well as the loads carried directly on the control surface. Since $(C_{N_\delta})_a$ has been previously determined independently from the hinge-moment data (fig. 9(a)), a measure of the control carry-over loading (in percent) could be obtained and is presented in figure 11(b). These values are much lower than linear theory would indicate and show the difference between the two plan forms to be a maximum of 15 percent near a Mach number of 0.70.

CONCLUSIONS

A free-flight investigation has been made with a rocket-powered model equipped with half-diamond tip controls (hinge lines located at 50.7 and 55.6 percent control root chords) on a 60° sweptback diamond wing having 30° sweptforward trailing edges. The following conclusions are drawn from the results obtained between Mach numbers of 0.50 and 1.30:

1. Control hinge moments, although very nonlinear in the transonic range, were relatively small throughout the speed range for all combinations of control deflection and angle of attack tested.

2. The center of pressure of the control-deflection loading c.p.$_\delta$ had a subsonic location of about 35 percent control mean aerodynamic chord $\bar{c}_a$ and a supersonic location that increased from $40\frac{1}{2}$ to $45\frac{1}{2}$ percent $\bar{c}_a$. The effect of an angle-of-attack range of ±3° was an irregular rearward shift in the supersonic value of c.p.$_\delta$, the mean level of which was about 45 percent $\bar{c}_a$.

3. The center of pressure of the control angle-of-attack loading c.p.$_\alpha$, near zero angle of attack, had mean locations of about 31 percent $\bar{c}_a$ subsonically and 41 percent $\bar{c}_a$ at supersonic speeds for zero control deflection. An angle-of-attack range of ±3° resulted in an irregular change in the variation of c.p.$_\alpha$ over the entire speed range presented and illustrated the nonlinear effect of the angle-of-attack range on c.p.$_\alpha$.

4. Values of control normal force per unit angle of attack were roughly twice as large as comparable values of control normal force per unit deflection. At supersonic speeds, 70 to 90 percent of the total normal force developed by control deflection was carried on the control surfaces, the remaining 10 to 30 percent being induced on the wing-model combination.

[redacted]

5. When a half-delta and a half-diamond tip control were compared, it was found that the half-diamond plan form produced more lift per unit angle of attack and a more forward (5 percent $\bar{c}_a$) c.p.$_\delta$ than the half-delta shape at all Mach numbers tested.

Langley Aeronautical Laboratory,
National Advisory Committee for Aeronautics,
Langley Field, Va., March 1, 1954.

REFERENCES

1. Lord, Douglas R., and Czarnecki, K. R.: Recent Information on Flap and Tip Controls. NACA RM L53I17a, 1953.

2. Conner, D. William, and May, Ellery B., Jr.: Control Effectiveness and Hinge-Moment Characteristics of a Tip Control Surface on a Low-Aspect-Ratio Pointed Wing at a Mach Number of 1.9. NACA RM L9H26, 1949.

3. Martz, C. William, Church, James D., and Goslee, John W.: Rocket-Model Investigation To Determine the Force and Hinge-Moment Characteristics of a Half-Delta Tip Control on a 59° Sweptback Delta Wing Between Mach Numbers of 0.55 and 1.43. NACA RM L52H06, 1952.

4. Martz, C. William, Church, James D., and Goslee, John W.: Free-Flight Investigation To Determine Force and Hinge-Moment Characteristics at Zero Angle of Attack of a 60° Sweptback Half-Delta Tip Control on a 60° Sweptback Delta Wing at Mach Numbers Between 0.68 and 1.44. NACA RM L51I14, 1951.

5. Lawrence, H. R.: The Lift Distribution on Low Aspect Ratio Wings at Subsonic Speeds. Jour. Aero. Sci., vol. 18, no. 10, Oct. 1951, pp. 683-695.

6. Cohen, Doris: Formulas for the Supersonic Loading, Lift, and Drag of Flat Swept-Back Wings With Leading Edges Behind the Mach Lines. NACA Rep. 1050, 1951.

[redacted]

TABLE I. - EXPERIMENTAL ANGLE-OF-ATTACK, CONTROL-SURFACE-DEFLECTION, AND CONTROL-HINGE-MOMENT DATA

M = 0.50					M = 0.60					M = 0.70				
C_{h_1}	δ_1	C_{h_2}	δ_2	α	C_{h_1}	δ_1	C_{h_2}	δ_2	α	C_{h_1}	δ_1	C_{h_2}	δ_2	α
0.0223	7.44	0.0676	6.30	13.43	-0.0125	9.77	-0.0250	7.65	- 4.99	0.0618	12.09	0.0994	10.31	5.35
.0282	8.79	.0751	7.37	13.26	.0043	10.71	-.0228	8.30	- 7.39	.0433	12.06	.0739	10.06	2.84
.0313	9.98	.0866	8.35	12.59	.0166	11.38	-.0195	8.77	- 9.71	.0197	11.27	.0335	9.11	.05
.0378	10.83	.0980	9.04	11.74	.0178	11.63	-.0261	8.89	-11.60	.0031	9.90	-.0015	7.65	- 2.53
.0448	11.44	.0998	9.49	10.47	.0169	11.71	-.0257	8.92	-12.81	-.0131	8.04	-.0297	5.93	- 5.12
.0499	11.77	.1059	9.78	8.75	.0182	11.44	-.0194	8.74	-13.69	-.0090	6.08	-.0452	4.14	- 7.60
.0580	11.88	.1054	9.83	6.93	.0092	10.63	-.0246	8.06	-14.13	-.0109	3.59	-.0667	1.93	- 9.69
.0486	11.73	.0876	9.58	4.90	.0064	9.45	-.0252	7.07	-14.09	-.0200	.89	-.0611	- .08	-11.09
.0391	11.15	.0630	8.96	2.72	.0014	8.06	-.0326	5.92	-13.63	-.0087	- 1.70	-.0704	- 2.31	-11.80
.0179	10.30	.0337	8.16	.62	-.0014	6.48	-.0421	4.59	-12.64	-.0186	- 4.45	-.0856	- 4.55	-11.71
.0021	9.12	.0071	7.10	- 1.32	-.0064	4.62	-.0670	2.93	-11.36	-.0240	- 6.95	-.0995	- 6.61	-10.85
-.0079	7.87	-.0166	5.98	- 3.40	-.0159	2.57	-.0684	1.34	- 9.53	-.0385	- 9.14	-.1217	- 8.46	- 9.14
-.0184	6.34	-.0337	4.71	- 5.55	-.0208	.46	-.0666	- .28	- 7.41	-.0492	-10.78	-.1386	- 9.79	- 6.99
-.0171	4.71	-.0490	3.34	- 7.55	-.0267	- 1.65	-.0653	-1.89	- 5.03	-.0370	-11.58	-.1127	-10.13	- 4.34
-.0196	2.94	-.0598	1.87	- 9.43	-.0248	- 3.73	-.0519	-3.40	- 2.77	-.0165	-11.67	-.0675	- 9.78	- 1.49
-.0263	1.11	-.0621	.42	-11.09	-.0132	- 5.59	-.0255	-4.69	- .44	-.0010	-10.98	-.0216	- 8.75	1.37
-.0172	- .76	-.0515	-1.02	-12.44	.0002	- 7.27	.0001	-5.84	1.71	.0028	- 9.79	.0173	- 7.30	4.50
-.0180	- 2.65	-.0552	-2.51	-13.24	.0043	- 8.79	.0172	-6.89	4.02	-.0097	- 8.22	.0333	- 5.78	7.27
-.0251	- 4.61	-.0592	-4.03	-13.71	-.0077	-10.06	.0297	-7.68	6.24	-.0062	- 6.04	.0368	- 4.05	9.77
-.0294	- 6.28	-.0682	-5.34	-13.91	-.0192	-10.96	.0268	-8.28	8.32	.0076	- 3.39	.0579	- 1.84	11.56
-.0336	- 7.97	-.0795	-6.70	-13.75	-.0260	-11.43	.0180	-8.65	10.11	.0203	- .75	.0629	.19	12.50
-.0385	- 9.38	-.0907	-7.84	-13.28	-.0244	-11.53	.0194	-8.66	11.67	.0169	1.98	.0482	2.19	12.71
-.0410	-10.42	-.1018	-8.65	-12.49	-.0257	-11.05	.0197	-8.24	12.59	.0199	4.28	.0561	4.04	12.15
-.0440	-11.17	-.1158	-9.26	-11.25	-.0211	-10.19	.0204	-7.53	13.16	.0286	6.61	.0643	5.88	10.81
-.0546	-11.59	-.1203	-9.54	- 9.67	-.0125	- 8.88	.0256	-6.50	13.28	.0444	8.65	.0917	7.66	8.57
-.0538	-11.73	-.1192	-9.59	- 7.81	-.0047	- 7.24	.0261	-5.24	12.93	.0484	10.28	.0929	8.91	5.85
-.0530	-11.33	-.1093	-9.20	- 5.85	.0004	- 5.38	.0356	-3.73	12.17	.0367	11.21	.0699	9.45	2.91
-.0343	-10.47	-.0877	-8.43	- 3.74	.0100	- 3.32	.0498	-2.05	10.94	.0138	11.52	.0307	9.39	- .07
-.0192	- 9.37	-.0531	-7.39	- 1.66	.0172	- 1.13	.0560	- .32	9.12	-.0040	11.51	-.0014	9.10	- 3.13
-.0036	- 7.90	-.0200	-6.10	.42	.0198	1.02	.0562	1.35	7.07	-.0026	11.24	-.0175	8.68	- 6.16
.0061	- 6.32	.0095	-4.73	2.56	.0301	3.11	.0573	2.93	4.80	.0174	10.62	-.0208	7.93	- 9.03
.0161	- 4.63	.0322	-3.32	4.60	.0273	5.08	.0438	4.37	2.42	.0116	9.12	-.0375	6.54	-11.52
.0175	- 2.68	.0456	-1.71	6.57	.0107	6.73	.0209	5.54	.18					
.0182	- .77	.0516	- .19	8.37	-.0024	8.20	-.0017	6.57	- 2.14					
.0165	1.12	.0451	1.27	9.82	-.0101	9.44	-.0203	7.42	- 4.25					
.0131	2.95	.0451	2.70	11.03	-.0058	10.39	-.0301	8.05	- 6.46					
.0171	4.73	.0587	4.15	12.06										
.0247	6.52	.0632	5.53	12.66										
.0298	7.93	.0638	6.60	12.94										

TABLE I.- EXPERIMENTAL ANGLE-OF-ATTACK, CONTROL-SURFACE-DEFLECTION, AND CONTROL-HINGE-MOMENT DATA - Continued

M = 0.80					M = 0.85					M = 0.90				
C_{h_1}	δ_1	C_{h_2}	δ_2	α	C_{h_1}	δ_1	C_{h_2}	δ_2	α	C_{h_1}	δ_1	C_{h_2}	δ_2	α
-0.0086	- 4.64	-0.0272	- 3.81	.32	-0.0440	-11.95	-0.1189	-11.10	-4.06	-0.0116	-10.64	-0.0432	- 8.98	-2.39
-.0007	- 2.50	-.0027	- 1.80	.55	-.0470	-12.20	-.1183	-11.22	-3.84	.0072	- 8.91	-.0419	- 7.83	-1.60
.0130	- .17	.0215	.27	1.42	-.0440	-11.94	-.1149	-10.93	-3.36	.0010	- 6.96	-.0351	- 6.06	- .76
.0223	2.08	.0431	2.30	2.20	-.0274	-10.60	-.0999	- 9.71	-2.77	-.0008	- 4.66	-.0164	- 3.81	.09
.0269	4.09	.0585	4.06	2.96	-.0138	- 9.07	-.0699	- 8.10	-2.06	.0067	- 1.88	.0055	- 1.25	1.11
.0287	6.02	.0728	5.78	3.58	-.0123	- 7.18	-.0543	- 6.33	-1.24	.0124	.74	.0257	1.17	1.88
.0311	7.68	.0830	7.21	4.08	-.0075	- 4.93	-.0319	- 4.19	- .39	.0135	3.25	.0392	3.40	2.65
.0336	9.15	.0945	8.50	4.47	.0011	- 2.49	-.0076	- 1.91	.38	.0080	5.51	.0443	5.34	3.27
.0406	10.42	.1073	9.63	4.70	.0120	- .07	.0178	.33	1.19	-.0030	7.41	.0458	7.01	3.78
.0494	11.45	.1118	10.40	4.80	.0200	2.57	.0406	2.74	2.00	.0066	9.36	.0510	8.51	4.00
.0497	11.91	.1083	10.69	4.61	.0242	4.84	.0547	4.71	2.65	.0258	10.96	.0851	10.22	4.07
.0538	12.18	.1086	10.86	4.36	.0242	6.86	.0668	6.51	3.22	.0230	11.71	.0860	10.85	3.90
.0538	12.29	.1063	10.85	3.98	.0279	8.60	.0772	8.00	3.67	.0250	11.97	.0821	10.94	3.48
.0534	11.94	.0961	10.40	3.40	.0487	10.49	.0985	9.62	3.93	.0252	11.93	.0759	10.71	2.87
.0367	10.90	.0762	9.36	2.71	.0490	11.45	.1017	10.42	4.02	-.0006	10.62	.0493	9.42	2.10
.0265	9.74	.0596	8.24	1.93	.0479	12.06	.1020	10.90	3.91	-.0017	9.27	.0335	7.94	1.25
.0206	8.29	.0434	6.87	1.10	.0476	12.30	.1023	11.11	3.62	.0010	7.64	.0227	6.35	.35
.0133	6.68	.0248	5.37	.25	.0520	12.36	.0972	10.94	3.16	.0001	5.63	.0036	4.35	- .60
.0048	4.77	.0046	3.62	- .59	.0469	11.68	.0644	9.81	2.59	-.0066	3.15	-.0229	1.89	-1.58
-.0079	2.62	-.0198	1.64	-1.54	.0246	10.22	.0540	8.66	1.91	-.0165	.45	-.0491	- .66	-2.52
-.0182	.53	-.0427	- .28	-2.40	.0184	8.77	.0405	7.30	1.16	-.0155	- 2.02	-.0605	- 2.86	-3.32
-.0261	- 1.53	-.0614	- 2.11	-3.22	.0135	6.93	.0251	5.61	.34	-.0084	- 4.50	-.0675	- 5.03	-4.07
-.0290	- 3.63	-.0753	- 3.93	-3.82	.0064	4.71	.0050	3.56	- .54	-.0054	- 6.60	-.0774	- 6.92	-4.57
-.0307	- 5.60	-.0861	- 5.61	-4.40	-.0079	2.37	-.0209	1.39	-1.42	-.0258	- 8.98	-.1038	- 9.04	-4.83
-.0334	- 7.39	-.0978	- 7.16	-4.89	-.0212	- .08	-.0453	- .85	-2.17	-.0264	-10.52	-.1034	-10.18	-4.91
-.0415	- 9.08	-.1086	- 8.56	-5.18	-.0254	- 2.59	-.0628	- 3.08	-2.96	-.0250	-11.38	-.0985	-10.70	-4.76
-.0501	-10.42	-.1178	- 9.63	-5.31	-.0254	- 4.58	-.0749	- 5.06	-3.58	-.0275	-11.91	-.0987	-11.04	-4.41
-.0530	-11.39	-.1296	-10.48	-5.32	-.0275	- 6.86	-.0877	- 6.83	-4.18	-.0321	-11.87	-.1034	-10.98	-3.85
-.0513	-11.93	-.1303	-10.89	-5.12	-.0343	- 8.76	-.1022	- 8.48	-4.54	-.0305	-10.97	-.0913	- 9.98	-3.06
-.0522	-12.14	-.1284	-11.00	-4.77	-.0494	-10.43	-.1225	- 9.95	-4.74	-.0063	- 9.16	-.0577	- 8.13	-2.18
-.0501	-12.08	-.1226	-10.84	-4.28	-.0472	-11.46	-.1249	-10.76	-4.70	-.0051	- 7.01	-.0453	- 6.20	-1.17
-.0462	-11.33	-.1020	- 9.91	-3.64	-.0457	-12.05	-.1247	-11.19	-4.53	-.0049	- 4.63	-.0221	- 3.84	- .12
-.0344	-10.24	-.0861	- 8.86	-2.92	-.0470	-12.20	-.1231	-11.20	-4.14	-.0059	- 2.03	.0069	- 1.32	.90
-.0237	- 8.83	-.0654	- 7.54	-2.15	-.0474	-11.76	-.1192	-10.75	-3.63	-.0167	.81	.0307	1.25	1.82
-.0181	- 7.13	-.0467	- 5.97	-1.36	-.0366	-10.58	-.0974	- 9.47	-2.98	.0181	3.48	.0447	3.61	2.82
-.0099	- 5.27	-.0231	- 4.20	- .44	-.0196	- 8.91	-.0715	- 7.89	-2.25					
.0007	- 3.18	-.0059	- 2.39	.52	-.0157	- 7.03	-.0537	- 6.12	-1.48					

TABLE I.- EXPERIMENTAL ANGLE-OF-ATTACK, CONTROL-SURFACE-DEFLECTION, AND CONTROL-HINGE-MOMENT DATA - Continued

M = 0.95					M = 1.00					M = 1.05				
C_{h_1}	δ_1	C_{h_2}	δ_2	α	C_{h_1}	δ_1	C_{h_2}	δ_2	α	C_{h_1}	δ_1	C_{h_2}	δ_2	α
0.0072	1.03	0.0241	1.51	2.45	0.0031	- 4.39	-0.0200	-3.89	-1.28	0.0392	- 5.47	-0.0274	- 6.19	-5.61
-.0031	3.49	.0294	3.72	3.31	.0023	- 1.44	-.0023	-1.04	.50	.0505	- 7.33	-.0238	- 7.75	-6.18
-.0186	5.65	.0291	5.65	4.10	.0033	1.59	.0149	1.82	1.53	.0585	- 8.73	-.0215	- 8.86	-6.45
-.0317	7.51	.0278	7.26	4.57	-.0061	4.16	.0217	4.18	2.41	.0598	- 9.55	-.0218	- 9.48	-6.33
-.0412	8.97	.0269	8.54	4.88	-.0198	6.30	.0236	6.15	3.24	.0519	- 9.81	-.0303	- 9.70	-5.82
-.0461	9.96	.0266	9.37	4.83	-.0300	8.11	.0244	7.77	3.70	.0311	- 9.50	-.0430	- 9.35	-4.80
-.0461	10.45	.0272	9.77	4.54	-.0382	9.45	.0239	8.95	3.96	.0206	- 7.97	-.0370	- 7.70	-3.48
-.0366	10.70	.0293	9.80	4.00	-.0427	10.18	.0226	9.56	3.98	.0119	- 5.73	-.0267	- 5.42	-1.98
-.0227	10.31	.0261	9.13	3.21	-.0400	10.46	.0244	9.77	3.78	.0044	- 2.98	-.0147	- 2.71	- .39
-.0185	9.05	.0227	7.90	2.20	-.0254	10.49	.0245	9.43	3.21	.0035	.11	.0089	.49	1.12
-.0096	7.38	.0169	6.24	.99	-.0206	9.40	.0212	8.30	2.48	-.0037	2.79	.0208	3.12	2.50
-.0038	5.26	.0047	4.16	- .26	-.0138	7.78	.0182	6.76	1.56	-.0211	5.14	.0238	5.40	3.85
-.0054	2.67	-.0186	1.54	-1.43	-.0047	5.72	.0116	4.76	.55	-.0347	7.05	.0239	7.17	4.75
-.0064	- .16	-.0423	-1.28	-2.65	-.0025	3.23	-.0032	2.33	- .55	-.0459	8.64	.0235	8.62	5.38
0047	- 2.73	-.0436	-3.48	-3.66	-.0037	.17	-.0254	- .72	-1.60	-.0514	9.60	.0233	9.47	5.65
.0206	- 5.07	-.0390	-5.45	-4.45	.0028	- 2.63	-.0364	-3.33	-2.53	-.0525	10.12	.0246	9.93	5.57
.0350	- 6.95	-.0366	-7.07	-5.05	.0153	- 5.06	-.0362	-5.42	-3.23	-.0407	10.37	.0305	10.01	5.02
.0460	- 8.55	-.0344	-8.42	-5.32	.0273	- 7.29	-.0323	-7.26	-3.80	-.0226	9.82	.0297	9.08	4.08
.0510	- 9.67	-.0318	-9.23	-5.29	.0379	- 8.86	-.0305	-8.60	-4.00	-.0171	8.30	.0253	7.56	2.96
.0505	-10.23	-.0324	-9.64	-5.05	.0433	- 9.84	-.0291	-9.35	-3.95	-.0099	6.34	.0181	5.62	1.63
.0395	-10.41	-.0390	-9.69	-4.46	.0436	-10.30	-.0277	-9.64	-3.61	-.0036	3.57	.0037	2.83	.11
.0288	- 9.67	-.0408	-8.90	-3.57	.0310	-10.28	-.0325	-9.43	-2.89	-.0029	.62	-.0189	- .24	-1.25
.0208	- 8.24	-.0347	-7.47	-2.59	.0233	- 9.26	-.0308	-8.37	-2.01	.0045	- 2.30	-.0320	- 3.08	-2.57
.0097	- 6.25	-.0300	-5.61	-1.39	.0157	- 7.46	-.0244	-6.62	-1.15	.0200	- 4.68	-.0329	- 5.26	-3.58
.0014	- 3.73	-.0147	-3.11	- .17	.0066	- 5.10	-.0163	-4.38	- .27	.0340	- 6.93	-.0311	- 7.23	-4.52
.0062	- .91	.0068	- .45	1.25	.0048	- 2.29	.0006	-1.66	.74	.0465	- 8.52	-.0283	- 8.61	-4.96
.0076	1.85	.0262	2.17	2.25	.0067	.76	.0169	1.15	1.78	.0526	- 9.49	-.0263	- 9.34	-4.83
-.0029	4.22	.0304	4.27	3.22	-.0013	3.31	.0239	3.46	2.56	.0511	- 9.99	-.0270	- 9.70	-5.01
-.0200	6.28	.0294	6.12	4.01	-.0151	5.71	.0249	5.61	3.17	.0330	-10.02	-.0420	- 9.71	-4.58
-.0328	7.85	.0287	7.52	4.53	-.0258	7.52	.0238	7.17	3.62	.0232	- 8.92	-.0394	- 8.49	-3.58
-.0416	9.23	.0277	8.71	4.85	-.0354	9.05	.0240	8.53	3.82	.0152	- 7.03	-.0323	- 6.62	-2.49
-.0472	10.05	.0273	9.43	4.93	-.0409	10.01	.0228	9.34	3.74	.0060	- 4.55	-.0244	- 4.25	-1.28
-.0470	10.43	.0275	9.71	4.73	-.0413	10.45	.0213	9.63	3.46	.0012	- 1.71	-.0072	- 1.38	.05
-.0363	10.62	.0315	9.73	4.25	-.0314	10.75	.0245	9.73	2.87	.0019	1.39	-.0113	1.60	1.15
-.0235	10.06	.0311	9.01	3.55	-.0216	10.07	.0196	8.82	2.09	-.0062	3.97	-.0204	4.04	1.81
					-.0161	8.72	.0156	7.46	1.22					

TABLE I.- EXPERIMENTAL ANGLE-OF-ATTACK, CONTROL-SURFACE-DEFLECTION, AND CONTROL-HINGE-MOMENT DATA - Concluded

M = 1.10					M = 1.20					M = 1.30				
C_{h_1}	δ_1	C_{h_2}	δ_2	α	C_{h_1}	δ_1	C_{h_2}	δ_2	α	C_{h_1}	δ_1	C_{h_2}	δ_2	α
0.0668	-8.42	-0.0136	-8.77	-8.66	-0.0222	10.16	0.0008	8.68	- .42					
.0661	-9.22	-.0154	-9.37	-7.20	-.0134	9.08	-.0106	6.91	-2.68	0.0178	-10.63	-0.0007	-8.91	2.49
.0521	-9.66	-.0267	-9.72	-5.72	.0006	7.22	-.0238	4.47	-5.13	.0074	-10.17	.0065	-7.74	3.82
.0280	-9.39	-.0363	-9.20	-3.84	.0210	5.18	-.0177	2.52	-7.24	.0017	- 8.46	.0102	-5.96	4.85
.0207	-7.73	-.0208	-7.12	-1.66	.0409	2.83	-.0057	.59	-8.66	-.0055	- 5.99	.0137	-3.58	5.56
.0109	-5.28	-.0045	-4.37	.55	.0581	.21	-.0022	-1.80	-9.42	-.0151	- 3.10	.0134	-1.01	5.95
.0053	-2.35	.0179	-1.12	2.72	.0637	- 2.78	.0003	-4.16	-9.43	-.0271	- .22	.0110	1.54	5.92
-.0125	.28	.0227	1.54	4.70	.0673	- 5.26	-.0035	-6.35	-8.80	-.0319	2.78	.0114	4.06	5.35
-.0334	2.63	.0178	3.67	6.27	.0650	- 7.44	-.0086	-8.16	-7.38	-.0330	5.66	.0113	6.32	4.33
-.0495	4.96	.0131	5.70	7.40	.0550	- 8.92	-.0135	-9.18	-5.56	-.0329	7.73	.0076	7.74	2.88
-.0600	6.83	.0125	7.37	7.96	.0420	- 9.71	-.0164	-9.48	-3.32	-.0310	9.38	.0026	8.68	1.00
-.0639	8.34	.0134	8.65	7.98	.0264	- 9.74	-.0120	-8.78	- .69	-.0255	10.26	-.0016	8.96	- .78
-.0633	9.31	.0142	9.42	7.53	.0148	- 8.52	.0012	-6.86	1.93	-.0143	10.68	-.0054	8.63	-2.45
-.0571	9.27	.0191	9.76	6.42	.0063	- 6.42	.0153	-4.36	4.44	-.0079	9.91	-.0166	7.14	-4.11
-.0367	9.94	.0279	9.66	4.99	-.0179	- 4.29	.0164	-1.96	6.59	.0024	8.27	-.0196	5.28	-5.60
-.0211	9.01	.0200	8.19	3.08	-.0391	- 1.81	.0089	.26	8.25	.0123	6.08	-.0180	3.30	-6.51
-.0136	7.34	.0094	6.28	1.09	-.0581	.70	.0039	2.55	9.18	.0236	3.30	-.0090	1.14	-7.01
-.0070	4.96	-.0069	3.67	- .91	-.0639	3.84	.0005	4.71	9.30	.0379	.75	-.0059	-1.20	-6.99
-.0028	2.15	-.0300	.51	-2.98	-.0683	5.68	.0035	6.66	8.95	.0414	- 2.35	-.0072	-3.78	-6.40
.0158	- .46	-.0311	-2.01	-4.72	-.0670	7.62	.0069	8.27	7.76	.0407	- 5.33	-.0119	-6.31	-5.32
.0380	-2.90	-.0238	-4.15	-6.24	-.0584	8.99	.0121	9.31	6.14	.0377	- 7.87	-.0092	-8.01	-3.77
.0523	-5.24	-.0194	-6.13	-7.22	-.0452	9.80	.0157	9.73	4.03	.0351	- 9.34	-.0058	-8.82	-1.92
.0610	-7.34	-.0180	-7.89	-7.71	-.0295	10.08	.0084	9.11	1.51	.0284	-10.13	-.0043	-9.09	.00
.0639	-8.75	-.0178	-8.98	-7.66	-.0181	9.20	-.0021	7.56	-1.00	.0168	-10.09	-.0016	-8.43	2.06
.0637	-9.47	-.0191	-9.52	-7.12	-.0066	7.54	-.0226	5.02	-3.68	.0048	- 9.00	.0100	-6.53	4.00
.0516	-9.70	-.0304	-9.74	-6.07	.0093	5.55	-.0261	2.87	-5.79	-.0061	- 6.80	.0134	-4.27	5.62
.0313	-9.14	-.0415	-9.13	-4.60	.0293	3.31	-.0129	1.07	-7.70	-.0182	- 4.25	.0134	-1.86	6.82
.0185	-7.55	-.0294	-7.16	-2.87	.0530	1.00	-.0066	-1.14	-9.04	-.0332	- 1.46	.0057	.44	7.47
.0098	-5.22	-.0179	-4.73	-1.04	.0635	- 1.85	-.0025	-3.46	-9.59	-.0479	1.08	.0054	2.88	7.46
.0053	-2.28	.0026	-1.61	1.04	.0685	- 4.44	-.0023	-5.59	-9.44	-.0504	3.88	.0072	5.23	6.81
-.0005	.69	.0204	1.46	2.79	.0690	- 6.84	-.0066	-7.63	-8.68	-.0492	6.34	.0110	7.28	5.74
-.0181	3.17	.0229	3.85	4.32	.0657	- 8.34	-.0100	-8.77	-7.19	-.0432	8.44	.0110	8.72	4.12
-.0367	5.37	.0223	5.95	5.74	.0545	- 9.34	-.0148	-9.40	-5.56	-.0380	9.59	.0068	9.22	2.23
-.0506	7.16	.0195	7.54	6.39	.0367	- 9.80	-.0232	-9.52	-4.11	-.0302	10.16	.0016	9.08	.04
-.0585	8.62	.0178	8.79	6.27						-.0143	10.19	-.0062	8.16	-2.03
										-.0065	8.91	-.0205	6.10	-3.47

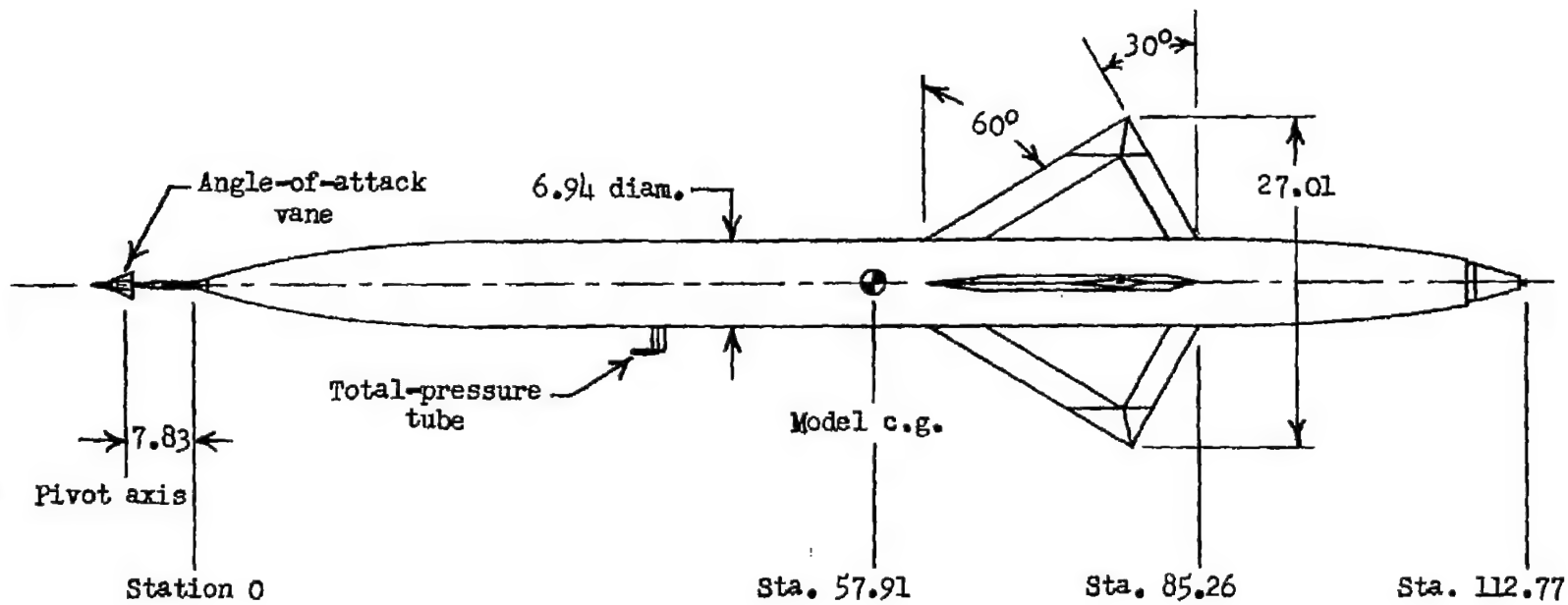

Model weight, 119.84 pounds

Figure 1.- General arrangement of the test vehicle. All dimensions are in inches unless otherwise noted.

(a) Plan view.

(b) Three-quarter view.

L-83341

Figure 2.- Photographs of test vehicle.

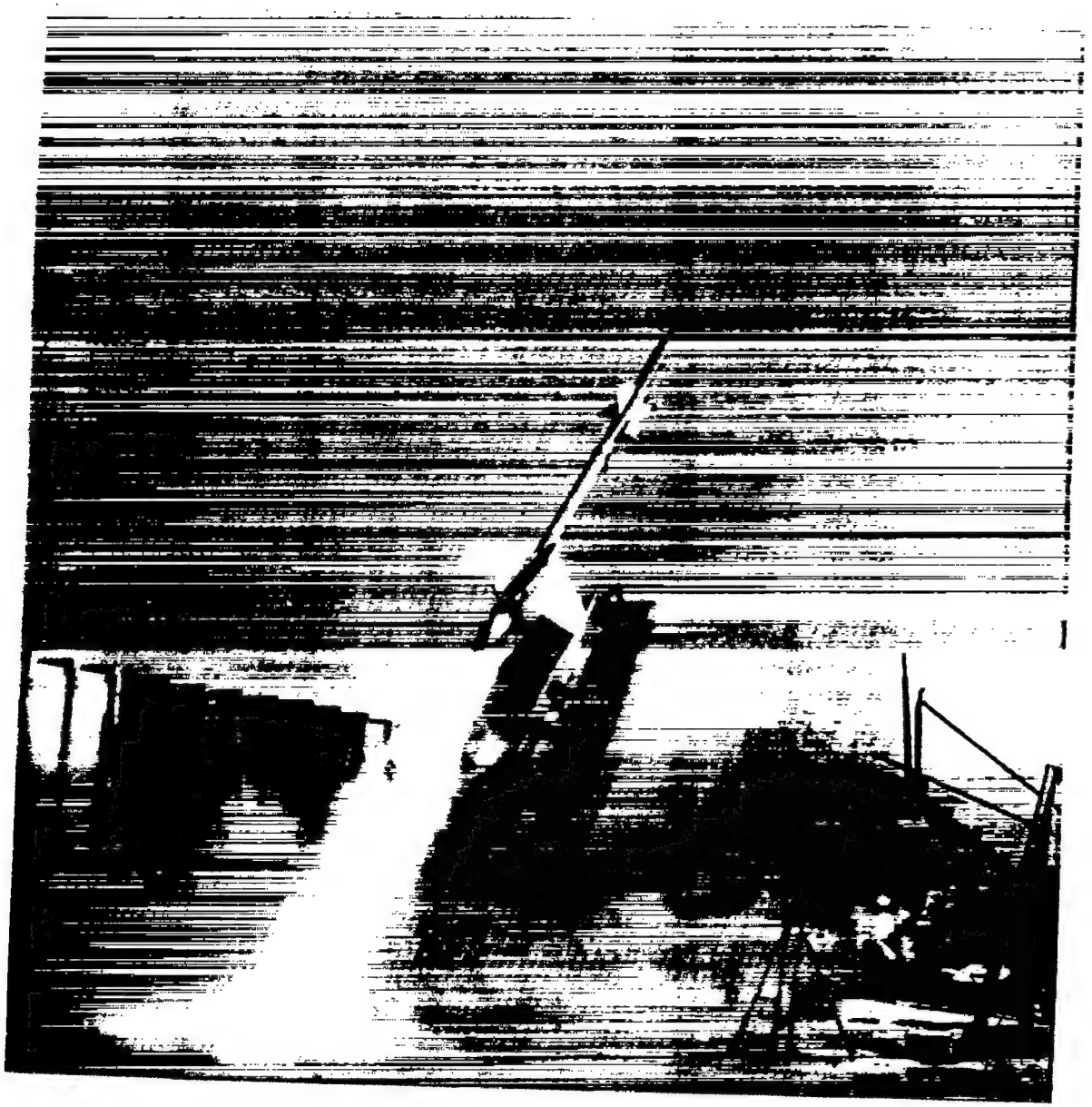

(c) Launching. L-75261

Figure 2.- Concluded.

[redacted]

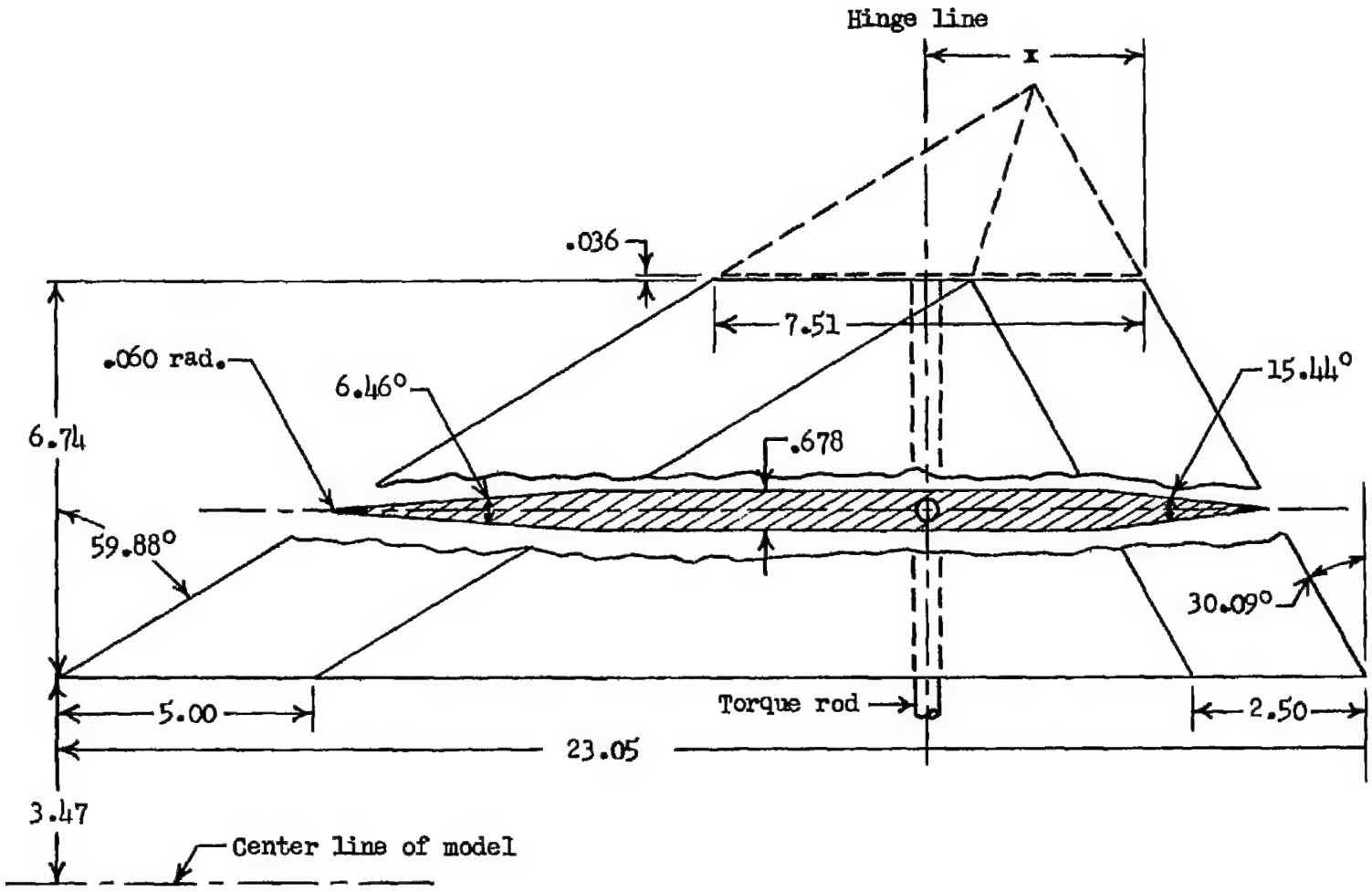

(a) Details of wing.

Figure 3.- Control wing geometry. All dimensions are in inches unless otherwise noted.

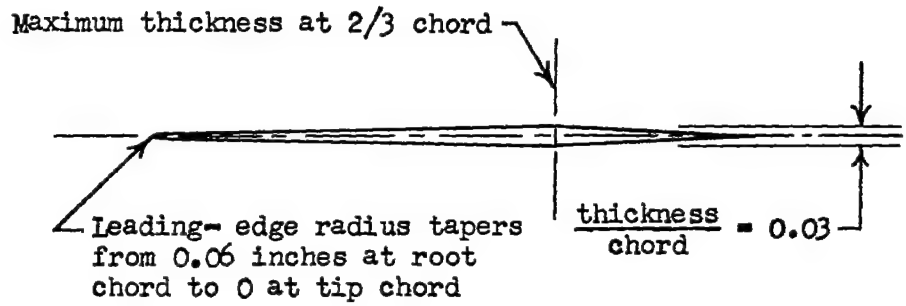

Section AA

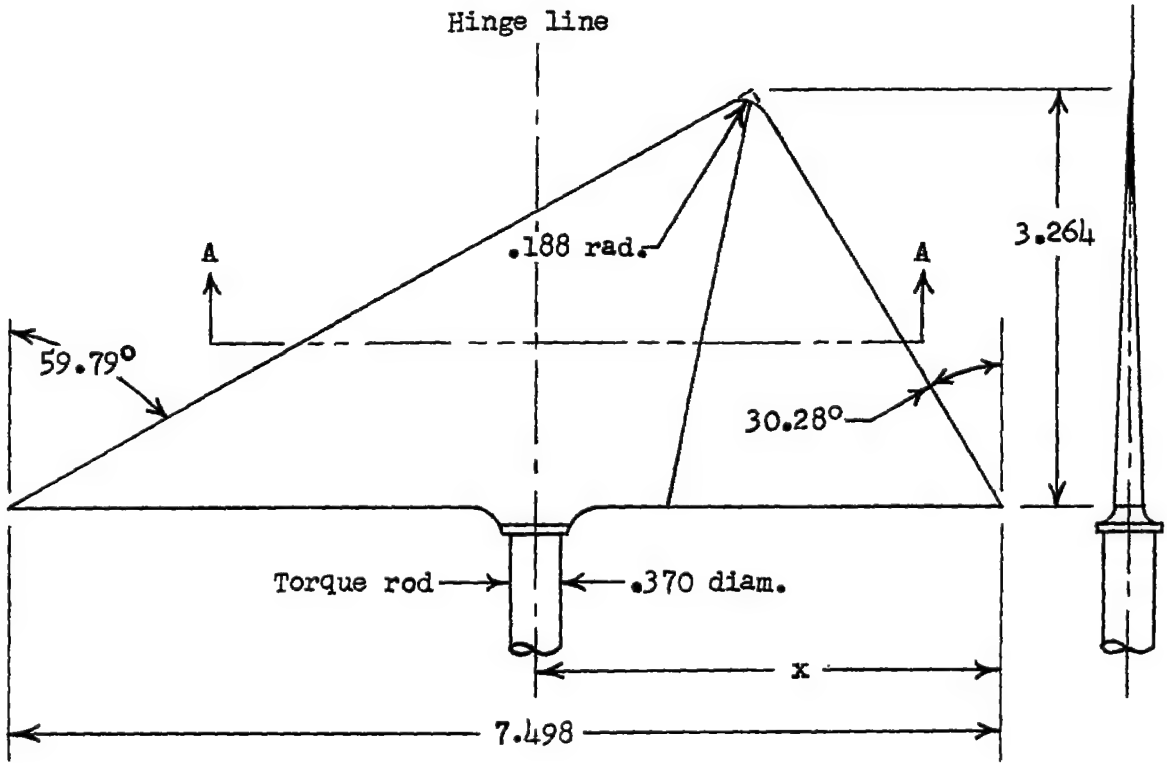

Control 1; x = 3.694 (hinge line at 0.5073 c_a or 0.3860 $\bar{c}_a$)
Control 2; x = 3.328 (hinge line at 0.5561 c_a or 0.4592 $\bar{c}_a$)

(b) Details of controls.

Figure 3.- Concluded.

[redacted]

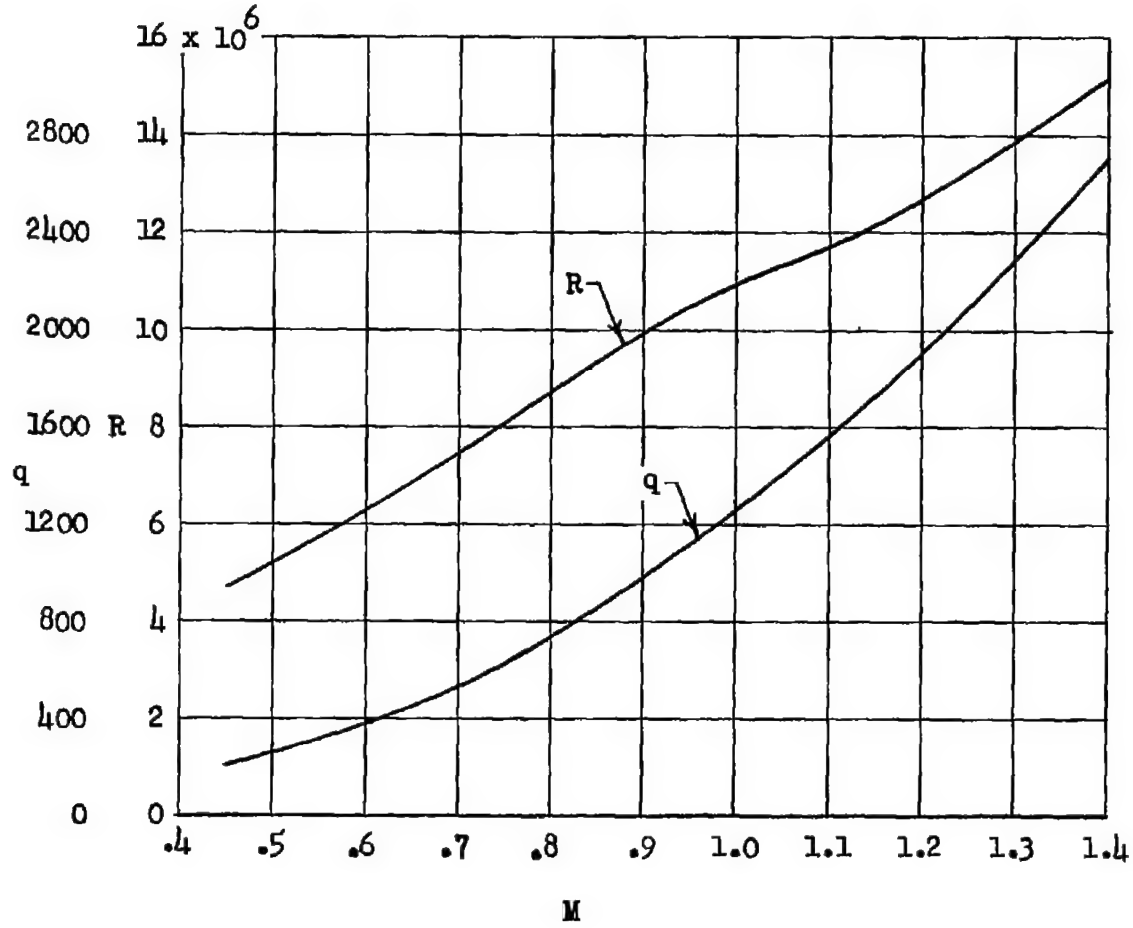

Figure 4.- Variation of Reynolds number and dynamic pressure with Mach number. Reynolds number is based on wing mean aerodynamic chord.

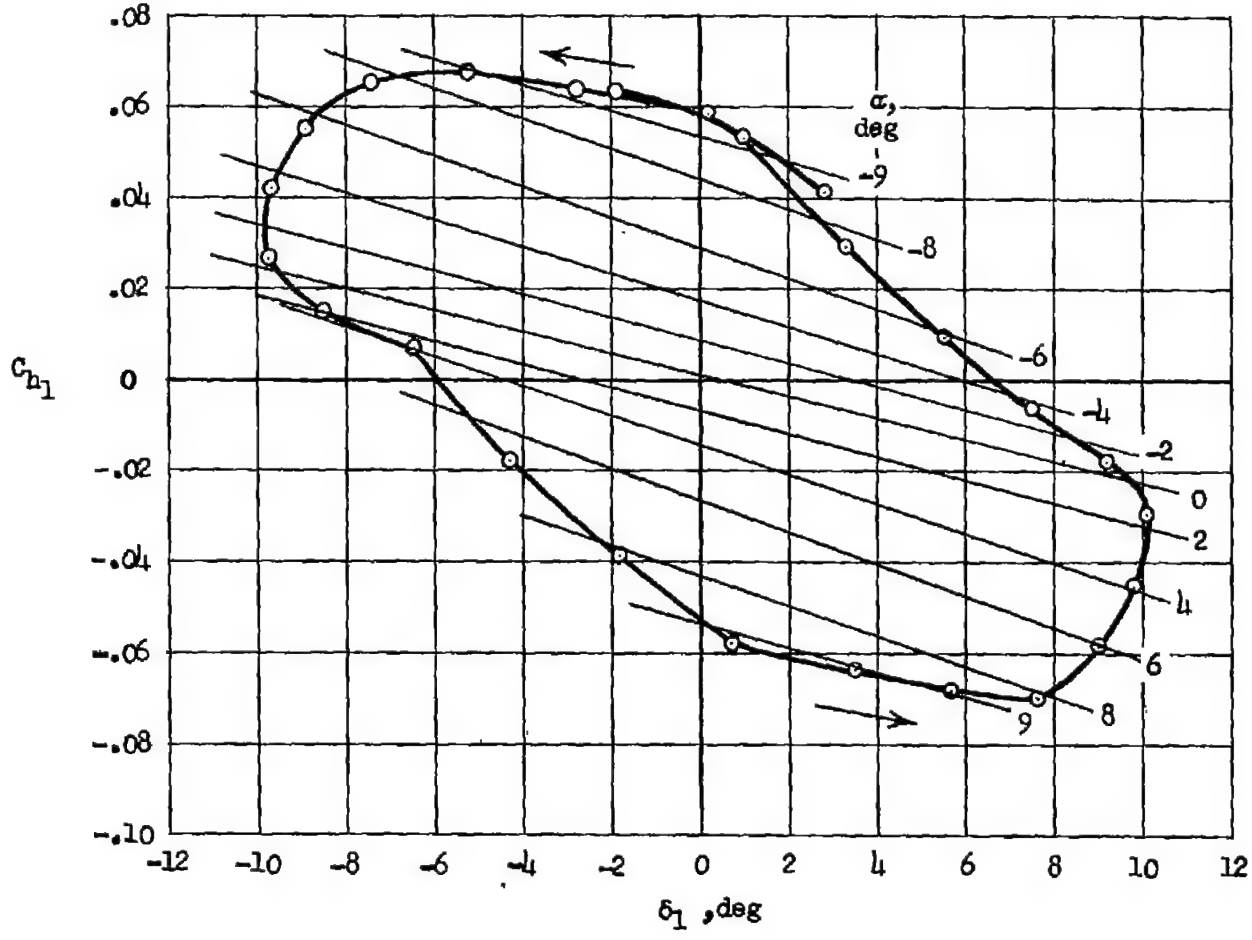

(a) Hinge-moment coefficient against control deflection.

Figure 5.- Sample hinge-moment-coefficient variation with control deflection and angle of attack. Hinge line at $0.5073c_a$; M = 1.20. The arrows indicate time sequence of recorded data.

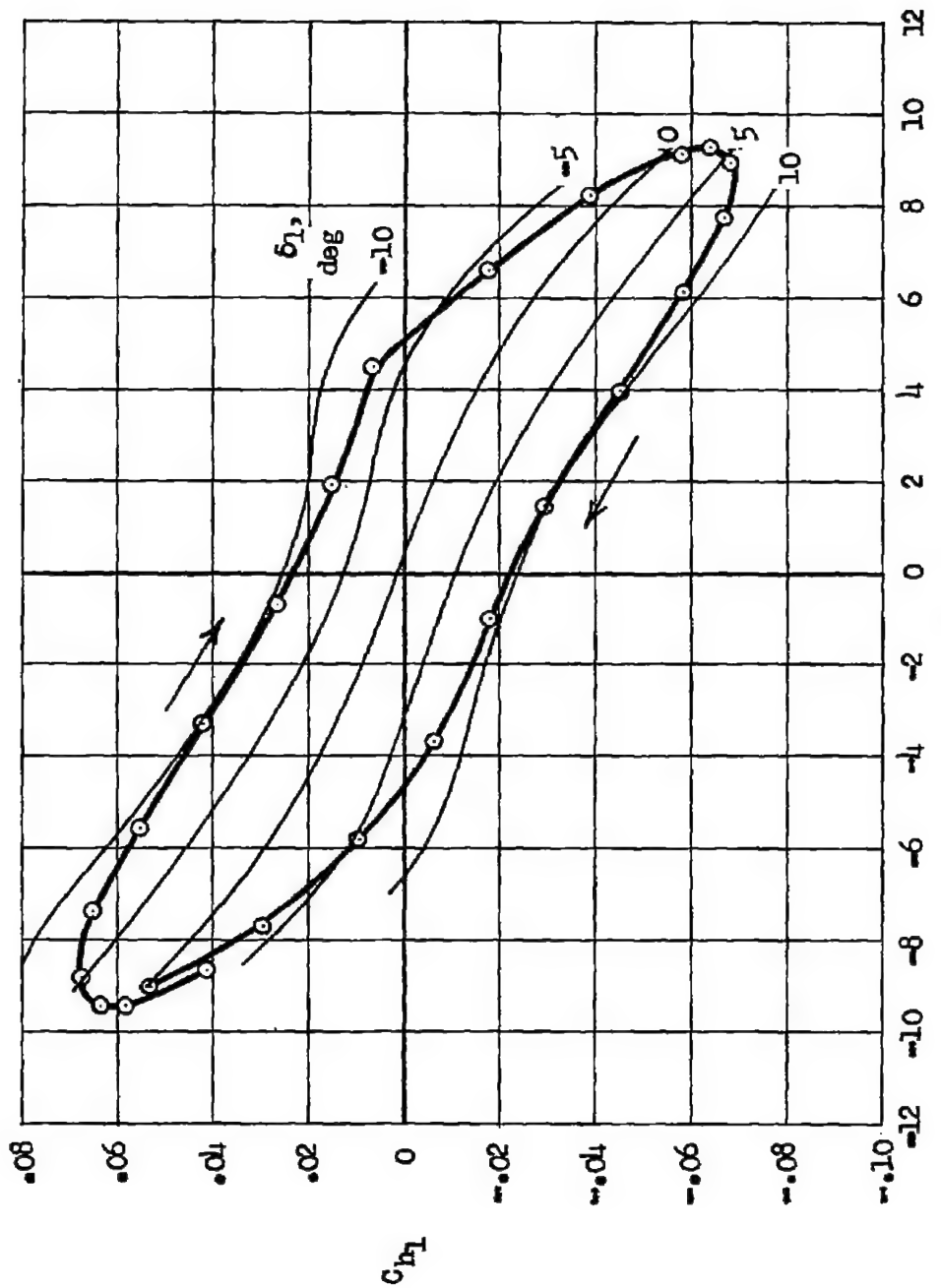

(b) Hinge-moment coefficient against angle of attack.

Figure 5.- Concluded.

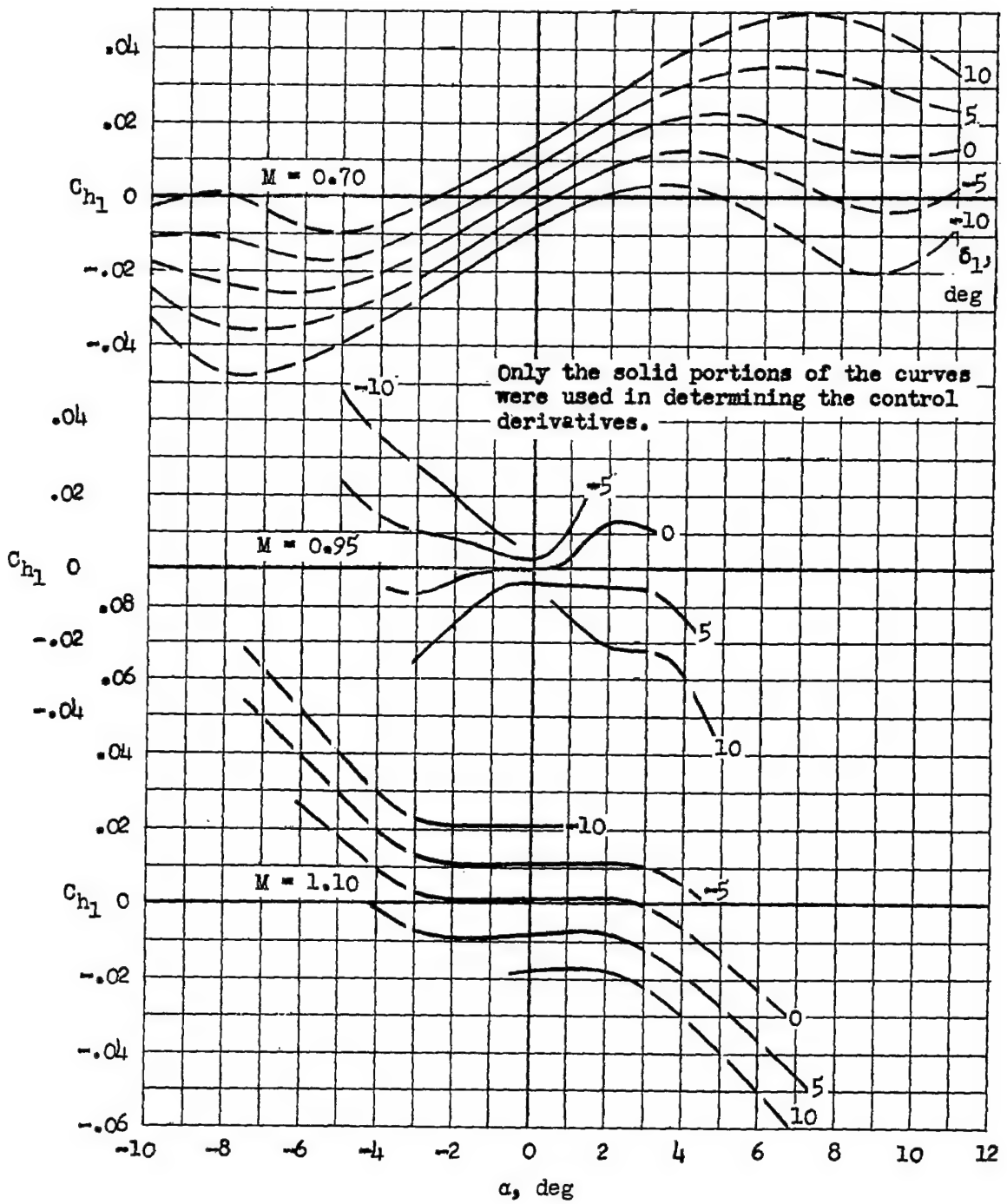

Figure 6.- Illustrative variation of faired hinge-moment coefficient with angle of attack at several control deflections and three Mach numbers. Hinge line at $0.5073c_a$.

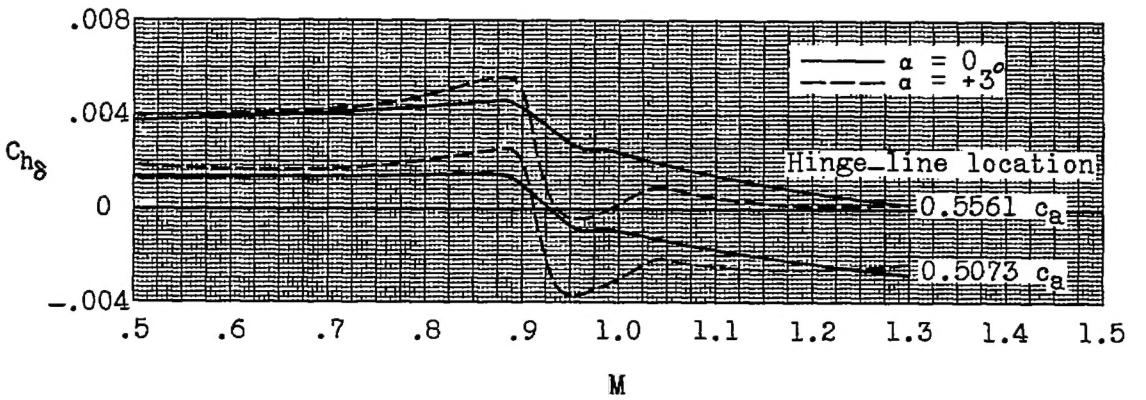

Figure 7.- The change in control-hinge-moment coefficient with respect to control deflection as a function of Mach number for the two hinge-line locations.

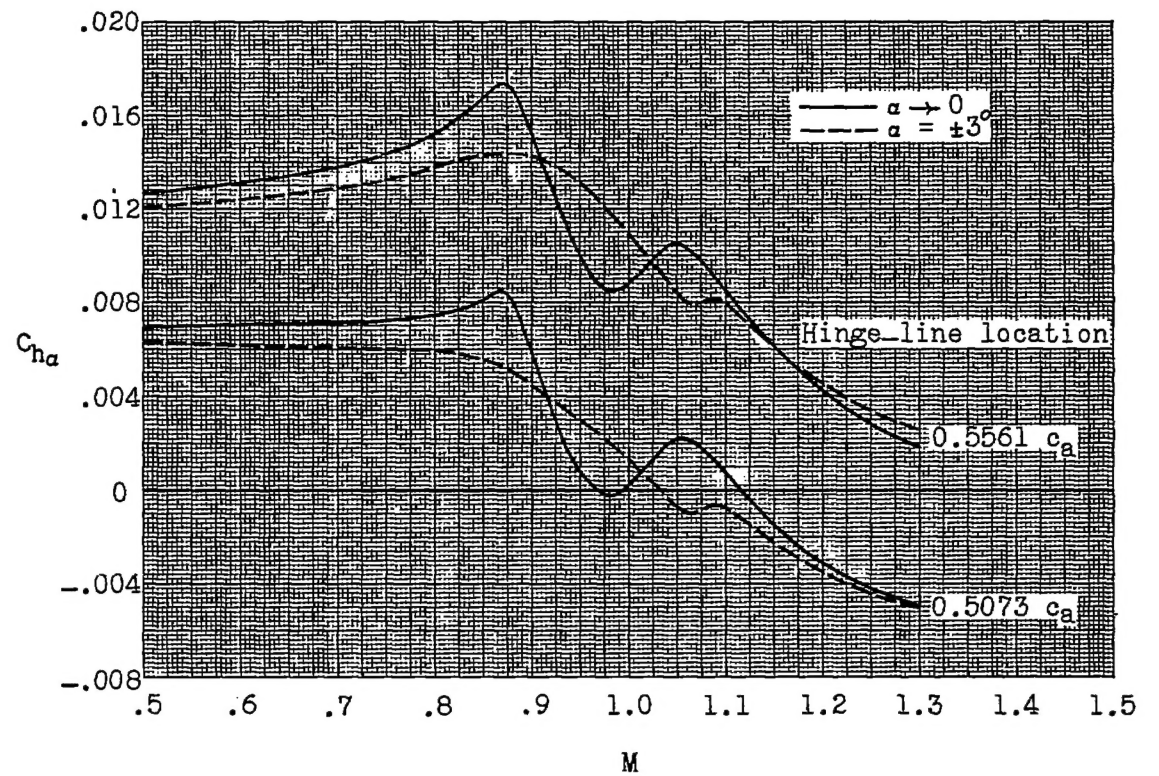

Figure 8.- The change in control-hinge-moment coefficient with respect to angle of attack as a function of Mach number for the two hinge-line locations. $\delta = 0$.

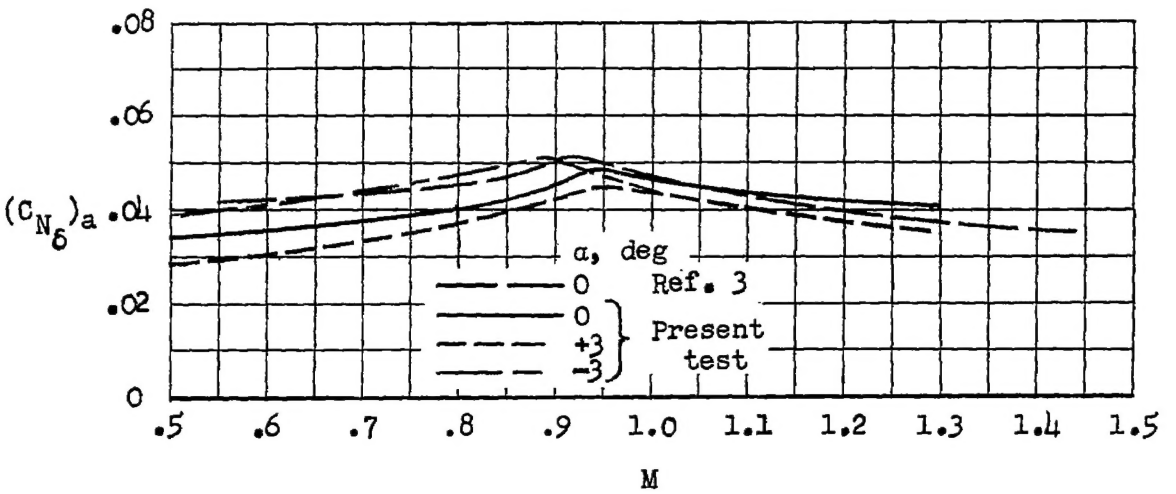

(a) Normal-force coefficient.

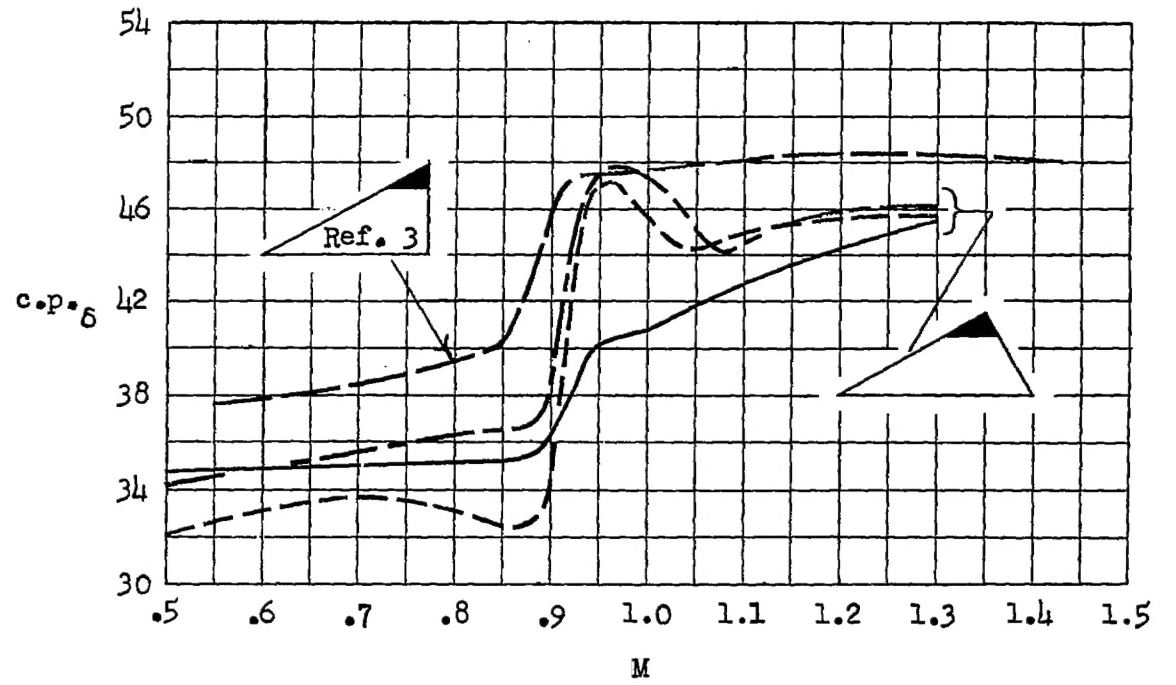

(b) Chordwise center-of-pressure location in percent $\bar{c}_a$.

Figure 9.- Mach number variation of the position and magnitude of the control forces due to control deflection.

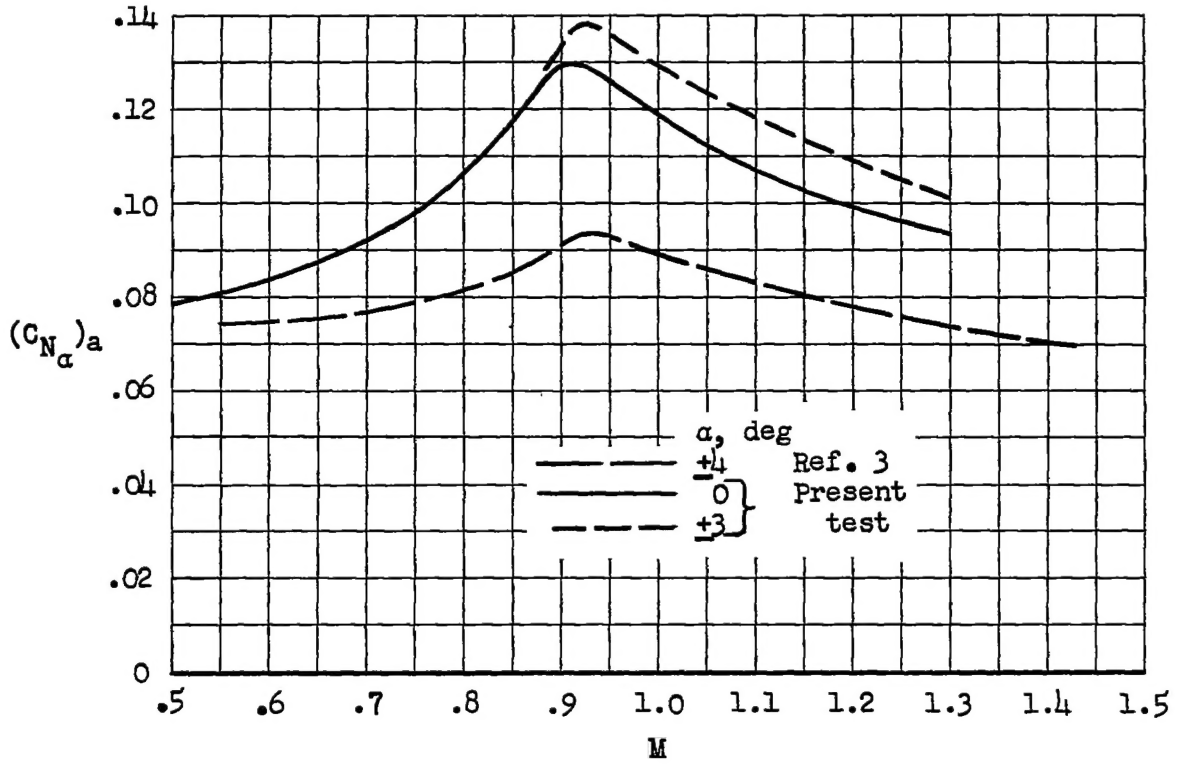

(a) Normal-force coefficient.

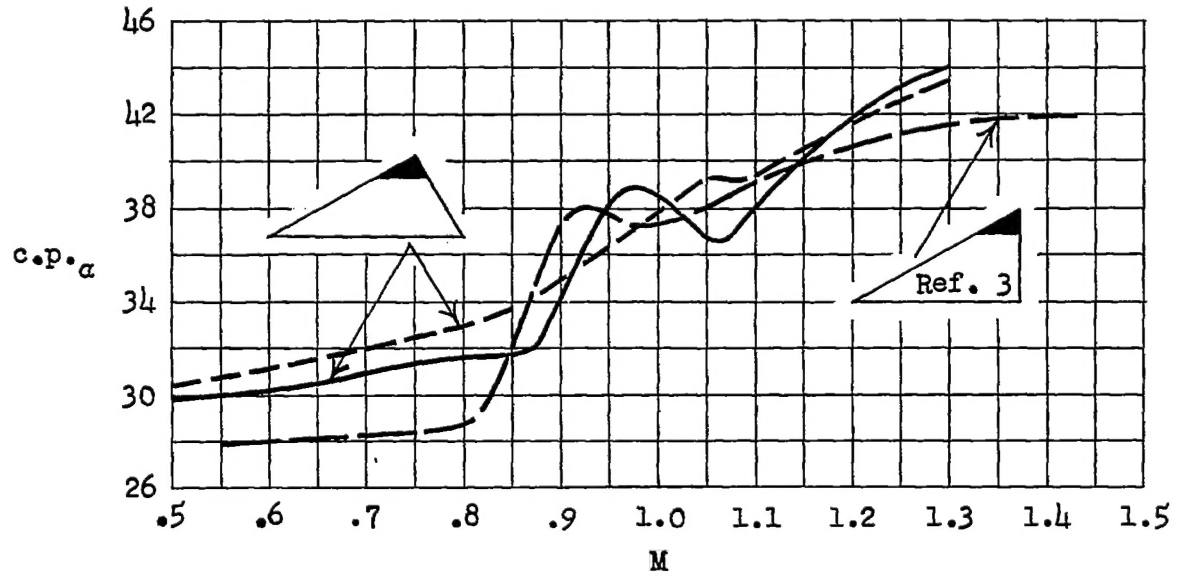

(b) Chordwise center-of-pressure location in percent $\bar{c}_a$.

Figure 10.- Mach number variation of the position and magnitude of the control forces due to angle of attack. $\delta = 0$.

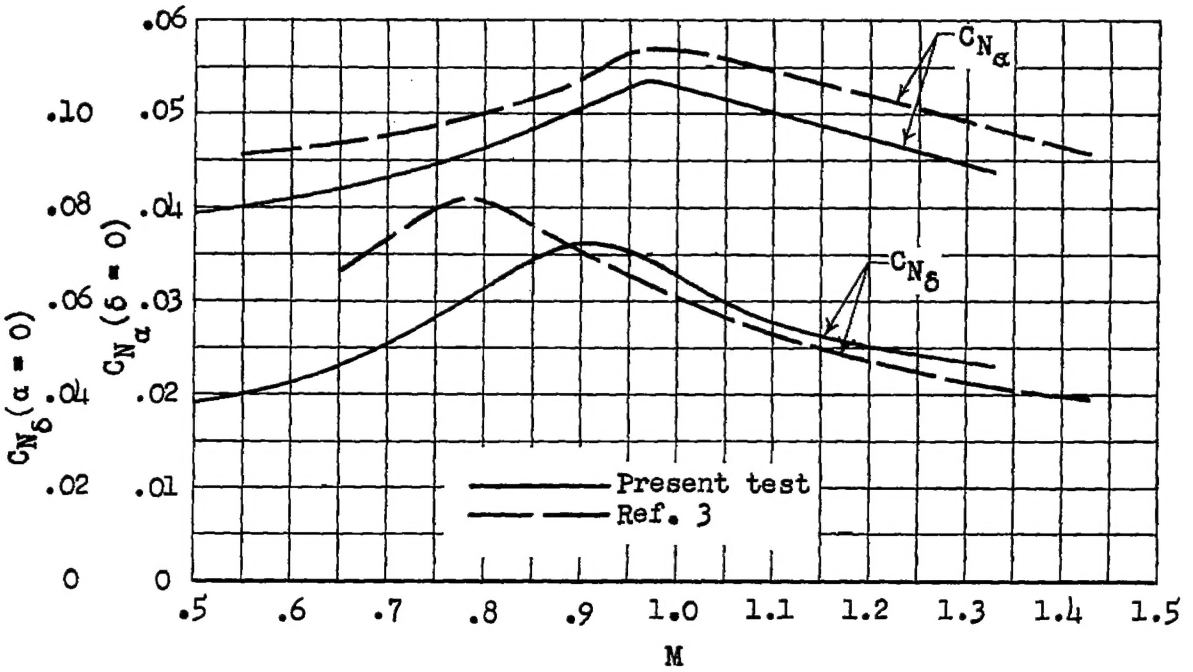

(a) Model normal-force-coefficient slope.

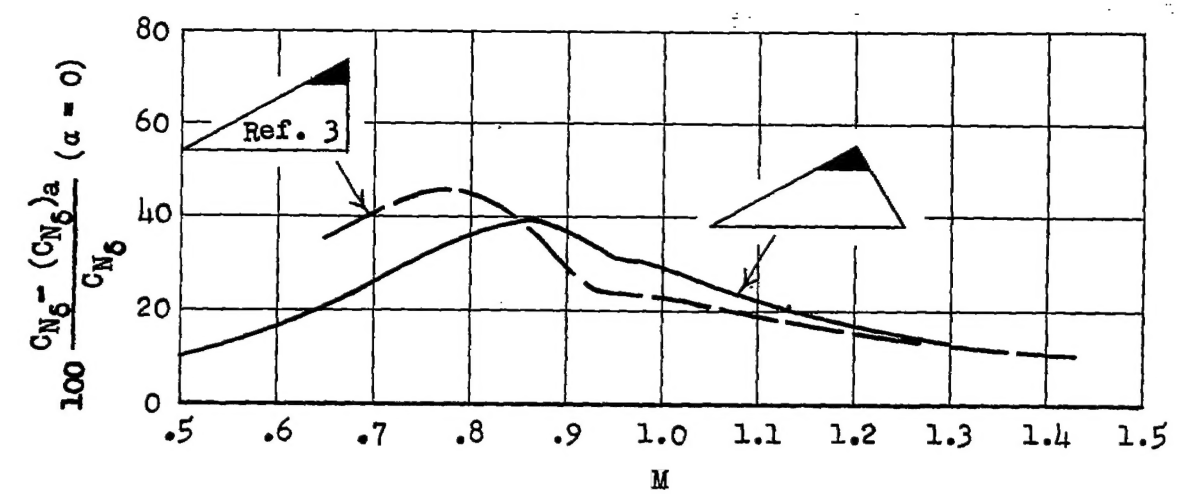

(b) Control "carry over" in percent.

Figure 11.- Model normal-force-coefficient slope with respect to angle of attack and control deflection and control "carry over" as functions of Mach number.

[redacted]

NACA-Langley - 4-26-54 - 300